

Chapter 1

Introduction: Hadrons as Systems of Constituent Quarks

Quantum chromodynamics, QCD, the theory of coloured quarks and gluons [1, 2], has a dual face. At small hadron distances ($r \ll 1$ fm) the quark–gluon interaction is weak; QCD is realised as a perturbative theory of QCD-quarks (or current quarks) and massless gluons. At distances of the order of hadron sizes ($r \sim 1$ fm) the interaction becomes strong and the perturbative description cannot be applied.

1.1 Constituent Quarks, Effective Gluons and Hadrons

Our present understanding of the quark–gluon structure of hadrons grew out, on the one hand, of the parton hypothesis [3, 4, 5] and, naturally, it is based on the experiments such as deep inelastic scatterings, e^+e^- annihilation, the production of $\mu^+\mu^-$ pairs and hadrons with large transverse momenta in high-energy hadron collisions. On the other hand, it is the result of the progress in quark models. Our knowledge is now based on quantum chromodynamics, the microscopic theory of strong interactions, which is a non-Abelian gauge theory of Yang–Mills fields [6]. The QCD-motivated quark models play a key role in the investigation of strong interactions.

Contrary to QED, where, along with the electron, there exists one neutral photon and the main process is the emission of photons by electrons, in QCD three types of quarks (three colours) are assumed, and each of them can transform into another via the emission of eight coloured gluons. The colour charge of gluons leads to the consequence that not only quarks emit gluons (Fig. 1.1a) but gluon emission by gluons (Fig. 1.1b) and gluon–gluon scattering (Fig. 1.1c) are also taking place. The requirement of three colours determines the theory unambiguously.

Quarks and gluons are not seen as free particles. In QCD there is

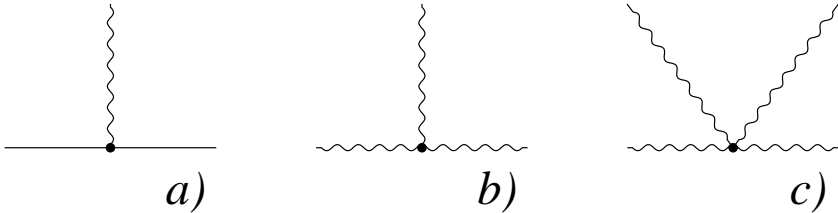


Fig. 1.1 QCD interaction vertices: gluon emission by a quark (a) or by a gluon (b); gluon–gluon scattering (c).

a confinement of coloured objects based on the increase of the effective charge at large distances. At the same time, non-Abelian gauge theories are asymptotically free [7, 8, 9], *i.e.* they are theories in which interactions at short distances are small. As a result, QCD gives a description of hard processes in a qualitative accordance with the interaction picture of the parton model.

At short distances, QCD is a well-defined renormalisable gauge theory [10]. The small value of the coupling constant at $r \rightarrow 0$ grants all the advantages of the developed technique of the Feynman diagrams in perturbation theory. The perturbative QCD (pQCD), providing a theoretical background for all the results obtained in the parton model, predicts at the same time certain deviations from the naive parton model in various hard processes. The reviews [11, 12, 13, 14, 15, 16] present a comprehensive analysis of the pQCD calculation technique and comparisons of the obtained results with experimental data.

Strong interactions change the properties of the quarks and gluons: the quark mass grows by 200 – 400 MeV, while the massless gluon turns into a massive effective gluon with $m_g \sim 700 - 1000$ MeV. Moreover, strong interactions may form new effective particles, *e.g.* composite systems of two quarks — diquarks. These can be either compact formations like constituent quarks or loosely bound systems of two quarks. Another possible class of effective particles could consist of coloured scalar mesons, which may be important in the formation of effective massive gluons.

There is one more highly important phenomenon in the region of strong interactions: the confinement of coloured particles. Coloured particles cannot occur at a distance more than 1–2 fm from each other. The only possibility to fly away (this is called deconfinement) is the formation process

of new quark–antiquark pairs followed by the production of new colourless objects: hadrons. Thus, quarks can get away from each other only as constituents of hadrons, *i.e.* if their colours are neutralised by other, newly produced quarks and gluons.

The idea that hadrons are not elementary particles is rather old: it appeared at the time when the first mesons were discovered. Fermi and Yang suggested that a pion consists of a proton and a neutron [17]. The discovery of the K -mesons gave rise to different versions of composite models. The common feature of these models was the assumption that the hadrons themselves were the constituents. In the late fifties the best known model of this kind was that of Sakata in which (p, n, Λ) are chosen as constituents, see *e.g.* [18, 19] and references in [19].

The suggestion of the quark structure of hadrons appeared first in the papers of Gell-Mann [20] and Zweig [21]. It was shown that the hadrons known at that time could be built up as composite systems of the three quarks (u, d, s) with fractional electric charges, obeying the rules of the $SU(3)$ symmetry. This was, in fact, the introduction of the constituent quarks. The quantum numbers of these three quarks (now we call them light quarks) are

<i>flavour</i>	<i>charge</i>	<i>isospin</i>	<i>baryon charge</i>	
u	$2/3$	$I = 1/2 \quad I_3 = 1/2$	$1/3$	(1.1)
d	$-1/3$	$I = 1/2 \quad I_3 = -1/2$	$1/3$	
s	$-1/3$	0	$1/3$	

The constituent (u, d) -quarks form an isotopic doublet and, thus, lead to the creation of hadronic isotopic multiplets.

Further, the notion of strangeness was introduced for hadrons built up from light quarks; the strangeness of the s -quark is taken to be -1 .

<i>flavour</i>	<i>strangeness</i>	
u	0	(1.2)
d	0	
s	-1	

If initially the quarks were understood just as a mathematical formulation of $SU(3)$ properties of hadrons [22, 23], soon it became clear that hadrons have to be considered as loosely bound systems of quarks. In the constituent quark picture of hadrons the meson consists of a quark–antiquark pair, while the baryons are systems of three constituent quarks:

$$M = \bar{q}q, \quad B = qq\bar{q}. \quad (1.3)$$

Let us underline that at those times only hadrons with small spins were known: mesons with $J^P = 0^-, 1^-$ and baryons with $J^P = 1/2^+, 3/2^+$. Attempts to discover free particles (quarks) with fractional electric charges failed [24]. The fact that quarks do not exist as experimentally observable particles is the phenomenon of quark confinement.

The introduction of the colour has a rather long history. Already when the quark model was constructed from constituent quarks (on the level of realisation of the $SU(3)$ symmetry), the introduction of new quark quantum numbers turned out to be necessary [25, 26, 27]. The picture of coloured quarks as we accept it now was formulated by Gell-Mann [1]. In this picture each quark possesses the quantum number of colour, which can have three values:

$$q_i \quad i = 1, 2, 3 \quad (\text{or red, green, blue}). \quad (1.4)$$

The coloured quarks realise the lowest representation of the colour group $[SU(3)]_{\text{colour}}$. It is postulated that the observable hadrons are singlets of the $[SU(3)]_{\text{colour}}$ group, *i.e.* they are white states. For the two-quark mesons and the three-quark baryons this means

$$M = \frac{1}{\sqrt{3}} \sum q_i \bar{q}_i, \quad B = \frac{1}{\sqrt{6}} \sum_{i,k,\ell} \varepsilon_{ik\ell} q_i q_k q_\ell. \quad (1.5)$$

Here the sum runs over the quark colours; $\varepsilon_{ik\ell}$ is the totally antisymmetric unit tensor.

Hence, the first historical step in understanding the quark–gluon nature of hadrons was the model of the constituent quark for the lowest hadrons, consisting of light quarks (1.1) with the new quantum number, the colour.

1.2 Naive Quark Model

The first successful steps in understanding the quark structure of hadrons were made in the framework of the non-relativistic quark model, especially when the $SU(6)$ symmetry was introduced. As time passed, it became obvious that this approach has restricted possibilities even for the lightest hadrons. Still, the simple picture given by the naive non-relativistic quark model provides us with a tool for the qualitative description of low-lying hadrons. Because of that, we present here the $SU(6)$ symmetry and its consequences in detail. In the end of the section we indicate those hadron properties which, obviously, cannot be handled in the framework of this description.

1.2.1 Spin–flavour $SU(6)$ symmetry for mesons

For the systematisation of hadrons, the $SU(6)$ symmetry was suggested in [28, 29]; this symmetry is a generalisation of $SU(4)$ which was used by Wigner for the description of nuclei [30].

Realising $SU(6)$ symmetry, the spin–flavour variables can be separated from the coordinate variables with a good accuracy. Hence, the wave functions can be written as

$$\Psi = C(\alpha(1), \bar{\alpha}(2))h(q(1), \bar{q}(2))\Phi_L(\mathbf{r}_1, \mathbf{r}_2) . \quad (1.6)$$

The colour part of the wave function $C(\alpha(1), \bar{\alpha}(2))$ is a common expression for all mesons, it is a colour singlet:

$$C(\alpha(1), \bar{\alpha}(2)) = \frac{1}{\sqrt{3}} \alpha_i(1)\bar{\alpha}_i(2) , \quad (1.7)$$

where the indices $i = 1, 2, 3$ describe the colours of the quark.

The spin–flavour part of the wave function $h(q(1)\bar{q}(2))$ realises a definite $SU(6)$ representation. In non-relativistic quark models an $SU(6)$ multiplet is characterized by the radial excitation quantum number (n) and the angular momentum (L). In the $SU(6)$ representation the standard notation for such a multiplet is $[N, L^P]_n$, where N is the total number of states in the multiplet (*i.e.* the dimension of the representation) and P is the parity of the states.

The coordinate part of the wave function $\Phi_L(\mathbf{r}_1, \mathbf{r}_2)$ is the same for all states of an $SU(6)$ multiplet. It is characterized by the total angular momentum L and its projection onto one of the axes, *e.g.* Z , *i.e.* L_Z :

$$\Phi_L(\mathbf{r}_1, \mathbf{r}_2) \longrightarrow Y_{LL_Z} \left(\frac{\mathbf{r}}{r} \right) \Phi_L(r) , \quad (1.8)$$

where $Y_{LL_Z}(\mathbf{r}/r)$ is a standard spherical function, and $\mathbf{r} = \mathbf{r}_1 - \mathbf{r}_2$, $r = |\mathbf{r}|$. The non-trivial coordinate part of the wave function $\Phi_L(r)$, which describes the dynamics of the state, depends on the distance between quarks. In what follows, we shall discuss the lightest multiplet with $L = 0$ and the next multiplet with $L = 1$ in terms of the $SU(6)$ symmetry. The radial quantum numbers of the considered multiplets are $n = 1$, *i.e.* they are basic states.

$SU(6)$ symmetry for the S-wave $q\bar{q}$ states

States with $L = 0$ and $n = 1$ are described by two $SU(6)$ multiplets: by the 35-plet $[35, 0^+]$ and the singlet $[1, 0^+]$ (we skip here the index corresponding to the radial quantum number).

The $[35, 0^+]$ multiplet contains the following states:

$$\begin{aligned} h_0 &= \pi^+, \pi^0, \pi^-, \eta^{(8)}, K^+, K^0, \bar{K}^0, K^-, \\ h_1 &= \rho^+, \rho^0, \rho^-, \omega, \phi, K^{*+}, K^{*0}, \bar{K}^{*0}, K^{*-} . \end{aligned} \quad (1.9)$$

The total number of states (1.9) is $8 + 3 \cdot 9 = 35$ (each vector state contains three states with different spin projections).

We have one $[1, 0^+]$ state, namely $\eta^{(1)}$.

The spin–flavour wave function projection of the singlet state $[1, 0^+]$ equals

$$|\eta^{(1)}\rangle = \frac{1}{\sqrt{6}} (u^\uparrow \bar{u}^\downarrow - u^\downarrow \bar{u}^\uparrow + d^\uparrow \bar{d}^\downarrow - d^\downarrow \bar{d}^\uparrow + s^\uparrow \bar{s}^\downarrow - s^\downarrow \bar{s}^\uparrow) . \quad (1.10)$$

This wave function is symmetrical in all flavour indices and antisymmetrical in the spin indices. It is a singlet in the flavour space and has a quark spin $S = 0$.

The wave function of the $[1, 0^+]$ state is written in a somewhat awkward form, because we use Clebsch–Gordan coefficients for constructing the spin wave function. We can see explicitly that $|\eta^{(1)}\rangle$ is an $SU(6)$ singlet, if we make use of the following spin functions for the quarks and antiquarks:

$$q_1 = \begin{pmatrix} q^\uparrow \\ 0 \end{pmatrix}, \quad q_2 = \begin{pmatrix} 0 \\ q^\downarrow \end{pmatrix}, \quad \bar{q}^1 = \begin{pmatrix} \bar{q}^\downarrow \\ 0 \end{pmatrix}, \quad \bar{q}^2 = \begin{pmatrix} 0 \\ -\bar{q}^\uparrow \end{pmatrix} . \quad (1.11)$$

In this case (1.10) can be rewritten as

$$|\eta^{(1)}\rangle = \frac{1}{\sqrt{6}} \sum_{q,a} q_a \bar{q}^a , \quad (1.12)$$

where the summation is carried out over $q = u, d, s$ and $a = 1, 2$. Following, however, the traditions of spectroscopy, we continue to use the Clebsch–Gordan coefficients even if this causes some inconvenience in writing the wave functions. The complete wave function of the $[1, 0^+]$ state (but without including the colour part) can be written as $|\eta^{(1)}\rangle \Phi_0^{(1)}(r)$. Let us now write the wave function of the 35-plet. First of all, consider the pseudoscalar particles h_0 from Eq. (1.9).

The wave function $|\eta^{(8)}\rangle$ is orthogonal to $|\eta^{(1)}\rangle$ in the flavour indices, it equals

$$|\eta^{(8)}\rangle = \frac{1}{2\sqrt{3}} (u^\uparrow \bar{u}^\downarrow + d^\uparrow \bar{d}^\downarrow - 2s^\uparrow \bar{s}^\downarrow - u^\downarrow \bar{u}^\uparrow - d^\downarrow \bar{d}^\uparrow + 2s^\downarrow \bar{s}^\uparrow) . \quad (1.13)$$

The wave functions of the π^+ - and π^0 -mesons are

$$\begin{aligned} |\pi^+\rangle &= \frac{1}{\sqrt{2}} (u^\uparrow \bar{d}^\downarrow - u^\downarrow \bar{d}^\uparrow) , \\ |\pi^0\rangle &= \frac{1}{2} (u^\uparrow \bar{u}^\downarrow - d^\uparrow \bar{d}^\downarrow - u^\downarrow \bar{u}^\uparrow + d^\downarrow \bar{d}^\uparrow) . \end{aligned} \quad (1.14)$$

The remaining wave functions of the pseudoscalar particles are obtained by the substitution of the indices in the π^+ -meson wave function: the wave function of the π^- -meson is the result of charge conjugation, $u \rightarrow \bar{u}$ and $\bar{d} \rightarrow d$. The wave function of the K^+ -meson can be obtained by substituting $\bar{d} \rightarrow \bar{s}$. We get the wave function of the K^0 -meson by the double substitution $u \rightarrow d$ and $\bar{d} \rightarrow \bar{s}$. The wave functions $|K^-\rangle$ and $|\bar{K}^0\rangle$ are given by the charge conjugation of $|K^+\rangle$ and $|K^0\rangle$.

We denote the spin-flavour wave functions with quark spin $S = 0$ as $|h_0\rangle$; let us repeat once more that this is $|\eta^{(8)}\rangle, |\pi^+\rangle, |\pi^0\rangle, \text{etc.}, \text{i.e.}$ all eight wave functions of the pseudoscalar mesons. The complete wave function of the 35-plet states with $S = 0$ is written as $|h_0\rangle \Phi_0^{(35)}(r)$. The wave functions of the h_1 -states of the 35-plet are the following. For the ρ^+ we have

$$|\rho_1^+\rangle = u^\uparrow \bar{d}^\uparrow, \quad |\rho_0^+\rangle = \frac{1}{\sqrt{2}} (u^\uparrow \bar{d}^\uparrow + u^\downarrow \bar{d}^\uparrow), \quad |\rho_{-1}^+\rangle = u^\downarrow \bar{d}^\uparrow. \quad (1.15)$$

The wave function of the ρ^- -meson can be obtained by the substitutions $u \rightarrow d, \bar{d} \rightarrow \bar{u}$ in (1.15), while the substitution $(u^a \bar{d}^b) \rightarrow (u^a \bar{u}^b - d^a \bar{d}^b) / \sqrt{2}$ in (1.15) gives the wave function of the ρ^0 -meson.

The substitution $\bar{d} \rightarrow \bar{s}$ in (1.15) leads to the K^{*+} -meson wave function; the wave function of K^{*0} is the result of the double substitution $u \rightarrow d, \bar{d} \rightarrow \bar{s}$.

The wave functions of the isoscalar vector states are

$$\begin{aligned} |\omega_1(n\bar{n})\rangle &= \frac{1}{\sqrt{2}} (u^\uparrow \bar{u}^\uparrow + d^\uparrow \bar{d}^\uparrow), \\ |\omega_0(n\bar{n})\rangle &= \frac{1}{2} (u^\uparrow \bar{u}^\downarrow + d^\uparrow \bar{d}^\downarrow + u^\downarrow \bar{u}^\uparrow + d^\downarrow \bar{d}^\uparrow), \\ |\omega_{-1}(n\bar{n})\rangle &= \frac{1}{\sqrt{2}} (u^\downarrow \bar{u}^\downarrow + d^\downarrow \bar{d}^\downarrow) \end{aligned} \quad (1.16)$$

and

$$|\phi_1(s\bar{s})\rangle = s^\uparrow \bar{s}^\uparrow, \quad |\phi_0(s\bar{s})\rangle = \frac{1}{\sqrt{2}} (s^\uparrow \bar{s}^\downarrow + s^\downarrow \bar{s}^\uparrow), \quad |\phi_{-1}(s\bar{s})\rangle = s^\downarrow \bar{s}^\downarrow. \quad (1.17)$$

Let us remind that the wave functions of the real mesons ω and ϕ are mixtures of pure $|\omega(n\bar{n})\rangle$ and $|\phi(s\bar{s})\rangle$ states of Eqs. (1.16) and (1.17). As a whole, we have 27 states with quark spins $S = 1$. We denote all spin-flavour wave functions of these states (given by (1.15)–(1.17) and similar formulae) as $|h_{1S_Z}\rangle$. The complete wave functions of the 35-plet with $S = 1$ can be written as $|h_{1J_Z}\rangle \Phi_0^{(35)}(r)$. The coordinate wave function coincides with that in $|h_0\rangle \Phi_0^{(35)}(r)$. Superpositions of $\eta^{(1)}$ and $\eta^{(8)}$ form observable η and η' mesons, they are mixed; this fact means that $\Phi_0^{(1)}(r)$ and $\Phi_0^{(35)}(r)$ are

sufficiently close to each other. That's why one speaks usually not about two multiplets, 1 and 35, but about one 36-plet.

SU(6) symmetry for the P-wave $q\bar{q}$ states

The application of SU(6) symmetry to P -wave $q\bar{q}$ states is not a flawless procedure since in P -wave mesons the relativistic effects cannot be small. Nevertheless, SU(6) symmetry is sometimes suitable for the description of such states. Let us, therefore, construct the wave functions.

States with $L \neq 0$ contain SU(6) multiplets $35 \otimes (2L+1)$ and $1 \otimes (2L+1)$. Hence, for $L = 1$ we have meson multiplets $[35 \otimes 3, 1^+]$ and $[1 \otimes 3, 1^+]$. The states belonging to these multiplets, the 35-plet and the axial singlet, are considerably mixed (in the same way as in the case of $L = 0$, when we observed the mixing of $\eta^{(1)}$ and $\eta^{(8)}$), and thus it is again reasonable to consider just a unique $(1 \oplus 35)$ -plet.

The spin-flavour part of the $L = 1$ meson wave functions is determined by the same functions $|\eta^{(1)}\rangle$, $|h_0\rangle$ and $|h_1\rangle$, as in the case of $L = 0$: the wave function of the $[1 \otimes 3, 1^+]$ multiplet can be written in the form

$$|\eta^{(1)}\rangle Y_{1L_z} \left(\frac{\mathbf{r}}{r} \right) \Phi_1^{(1)}(r). \quad (1.18)$$

The wave functions of the $[35 \otimes 3, 1^+]$ -plet with spin $S = 0$ are defined with the help of $|h_0\rangle$:

$$|h_0\rangle Y_{1L_z} \left(\frac{\mathbf{r}}{r} \right) \Phi_1^{(35)}(r). \quad (1.19)$$

We denote meson states related to this multiplet as b_1^+ , b_1^0 , b_1^- , $h_1^{(8)}$ ($I = 0$) and K_1 ($I = 1/2$), while for the wave functions with $S = 1$ we use $|h_{1S_z}\rangle$:

$$\sum_{L_z+S_z=J_z} C_{1L_z 1S_z}^{JJ_z} |h_{1S_z}\rangle Y_{1L_z} \left(\frac{\mathbf{r}}{r} \right) \Phi_1^{(35)}(r). \quad (1.20)$$

The corresponding meson states are denoted as a_J^+ , a_J^0 , a_J^- , $f_J(n\bar{n})$, $f_J(s\bar{s})$, K_J with $J = 0, 1, 2$.

It is reasonable to suppose that $\Phi_1^{(1)}(r)$ and $\Phi_1^{(35)}(r)$ nearly coincide, and we can consider a unique set of states $(1 \oplus 35) \otimes 3$.

Predictions for 36 - plets with $L = 1$ and the estimations of their masses were first given in [31, 32].

1.2.2 Low-lying baryons

Low-lying baryons, octets and decuplets in the terminology of $SU(3)_{flavour}$ symmetry, may also be described qualitatively in the framework of $SU(6)$ symmetry.

We have in mind the following baryons:

(i) the octet with $J^P = 1/2^+$:

isospin	strangeness	particles	
1/2	0	p, n	(1.21)
0	-1	Λ	
1	-1	$\Sigma^+, \Sigma^0, \Sigma^-$	
1/2	-2	Ξ^0, Ξ^- ;	

(ii) the decuplet with $J^P = 3/2^+$:

isospin	strangeness	particles	
3/2	0	$\Delta^{++}, \Delta^+, \Delta^0, \Delta^-$	(1.22)
1	-1	$\Sigma^{*+}, \Sigma^{*0}, \Sigma^{*-}$	
1/2	-2	Ξ^{*0}, Ξ^{*-}	
0	-3	Ω^- .	

Below, we discuss the description of the wave functions of these baryons in terms of the $SU(6)$ symmetry.

1.2.3 Spin-flavour $SU(6)$ symmetry for baryons

The baryons consist of three quarks qqq ; the colour part of the wave function is the same for all baryons

$$C(\alpha(1), \alpha(2), \alpha(3)) = \frac{1}{\sqrt{6}} \varepsilon_{ikl} \alpha_i(1) \alpha_k(2) \alpha_l(3). \quad (1.23)$$

Since the decuplet is antisymmetric with respect to any permutation of quarks, which obey Fermi statistics, the remaining part of the wave function (*i.e.* the coordinate and the spin-flavour one) should be exactly symmetric.

It seems to be natural that once the coordinate wave function $\Phi(\mathbf{r}_1, \mathbf{r}_2, \mathbf{r}_3)$ is completely symmetric for the lowest baryon states, the spin-flavour part must be also symmetric: this corresponds to the 56-plet representation of the $SU(6)$ group. If $\Phi(\mathbf{r}_1, \mathbf{r}_2, \mathbf{r}_3)$ is totally antisymmetric, the spin-flavour part has to be also antisymmetric (20-plet representation). $\Phi(\mathbf{r}_1, \mathbf{r}_2, \mathbf{r}_3)$ can be also of mixed symmetry (*i.e.* it corresponds to a mixed Young scheme): this leads to the mixed symmetry of the spin-flavour wave function, which corresponds to the 70-plet representation. All the baryons observed up to now seem to belong to either the 56-plet or the 70-plet; so far no states belonging to the 20-plet are established with certainty.

The 56-plet

Assembling the baryon wave functions, it is convenient to write the spin-flavour part $h(q(1), q(2), q(3))$ in the form of a direct product of the spin function $|SS_Z\rangle$ (where S is the total spin of three quarks, S_Z is its Z-projection) and the flavour function $|q_1q_2q_3\rangle$ (q_i are symbols of the u, d, s quarks). The symmetric spin functions (spin 3/2) are

$$\left| \frac{3}{2} \frac{3}{2} \right\rangle = \uparrow\uparrow\uparrow, \quad \left| \frac{3}{2} \frac{1}{2} \right\rangle = \frac{1}{\sqrt{3}} (\uparrow\uparrow\downarrow + \uparrow\downarrow\uparrow + \downarrow\uparrow\uparrow), \quad (1.24)$$

etc., for spin 1/2 (mixed symmetry) two orthogonal combinations can be written

$$\left| \frac{1}{2} \frac{1}{2} \right\rangle_\lambda = \frac{1}{\sqrt{6}} (\uparrow\uparrow\downarrow + \uparrow\downarrow\uparrow - 2\downarrow\uparrow\uparrow), \quad \left| \frac{1}{2} \frac{1}{2} \right\rangle_\rho = \frac{1}{\sqrt{2}} (\uparrow\uparrow\downarrow - \uparrow\downarrow\uparrow). \quad (1.25)$$

The SU(3) decuplet flavour function is symmetric:

$$\begin{aligned} |10\rangle &= \frac{1}{\sqrt{6}} (q_1q_2q_3 + q_1q_3q_2 \\ &\quad + q_2q_1q_3 + q_2q_3q_1 + q_3q_1q_2 + q_3q_2q_1) \text{ (three different flavours)} \\ &= \frac{1}{\sqrt{3}} (q_1q_1q_2 + q_1q_2q_1 + q_2q_1q_1) \text{ (two flavours coincide)}, \\ &= (q_1q_1q_1) \text{ (all flavours coincide)}. \end{aligned} \quad (1.26)$$

There are two orthogonal octet flavour functions with mixed symmetry (that is, at least two flavours must be different):

$$\begin{aligned} |8\rangle_\lambda &= \frac{1}{2\sqrt{3}} (q_1q_2q_3 + q_1q_3q_2 \\ &\quad + q_2q_1q_3 + q_2q_3q_1 - 2q_3q_1q_2 - 2q_3q_2q_1) \text{ (three different flavours)} \\ &= \frac{1}{\sqrt{6}} (q_1q_1q_2 + q_1q_2q_1 - 2q_2q_1q_1) \text{ (two flavours coincide)} \\ |8\rangle_\rho &= \frac{1}{2} (q_1q_2q_3 - q_1q_3q_2 - q_2q_3q_1 + q_2q_1q_3) \text{ (three different flavours)} \\ &= \frac{1}{\sqrt{2}} (q_1q_1q_2 - q_1q_2q_1) \text{ (two flavours coincide)}. \end{aligned} \quad (1.27)$$

Finally, the SU(3) singlet is antisymmetric; therefore, only the component with three different flavours survives:

$$|1\rangle = \frac{1}{\sqrt{6}} (q_1q_2q_3 + q_2q_3q_1 + q_3q_1q_2 - q_2q_1q_3 - q_3q_2q_1 - q_1q_3q_2). \quad (1.28)$$

All the functions (1.26–1.28) are normalised to unity.

The direct product of the spin and flavour functions forms the spin-flavour baryon wave function, *e.g.*

$$\begin{aligned}
 |8\rangle_\rho \left| \frac{1}{2} \frac{1}{2} \right\rangle_\lambda &= \frac{1}{2\sqrt{6}} (q_1^\uparrow q_2^\uparrow q_3^\downarrow + q_1^\uparrow q_2^\downarrow q_3^\uparrow - 2q_1^\downarrow q_2^\uparrow q_3^\uparrow - q_1^\uparrow q_3^\uparrow q_2^\downarrow - q_1^\downarrow q_3^\downarrow q_2^\uparrow + 2q_1^\downarrow q_3^\uparrow q_2^\uparrow \\
 &\quad - q_2^\uparrow q_3^\uparrow q_1^\downarrow - q_2^\downarrow q_3^\downarrow q_1^\uparrow + 2q_2^\downarrow q_3^\uparrow q_1^\uparrow + q_2^\uparrow q_1^\uparrow q_3^\downarrow + q_2^\downarrow q_1^\downarrow q_3^\uparrow - 2q_2^\downarrow q_1^\uparrow q_3^\uparrow) .
 \end{aligned} \tag{1.29}$$

The baryons of the lowest multiplet $[56, 0^+]_0$ have a totally symmetric coordinate part of the wave function — the orbital momentum of any quark pair equals zero. The spin-flavour part is also totally symmetric; to a symmetric flavour part (decuplet) corresponds the spin value $3/2$, to a flavour function of mixed symmetry (octet) the spin $1/2$:

$$[56, 0^+]_0 = {}^4 10_{3/2} + {}^2 8_{1/2} . \tag{1.30}$$

(We denote the SU(3) multiplets by ${}^{2s+1} H_J$, where J is the baryon spin and H stands for the number of states in the multiplet.) Hence,

$$\left| {}^4 10_{\frac{3}{2}} \right\rangle_{J_z} = |10\rangle \left| \frac{3}{2} J_z \right\rangle , \quad \left| {}^2 8_{\frac{1}{2}} \right\rangle_{J_z} = \frac{1}{\sqrt{2}} \left(|8\rangle_\lambda \left| \frac{1}{2} J_z \right\rangle_\lambda + |8\rangle_\rho \left| \frac{1}{2} J_z \right\rangle_\rho \right) . \tag{1.31}$$

The 70-plet

The coordinate part of the wave function of the multiplet with $L = 1$ is of mixed symmetry — only one quark pair is in a P -wave state. Because of that, the spin-flavour part should be also of mixed symmetry, *i.e.* we have a multiplet $[70, 1^-]_1$ [33]. The symmetric and antisymmetric flavour functions correspond here to the quark spin $1/2$, the mixed flavour function to spin $1/2$ or spin $3/2$. Combining the quark spins with the angular momenta, we can obtain the SU(3) multiplets:

$$\begin{aligned}
 [70, 1^-] &= {}^4 8_{5/2} + {}^4 8_{3/2} + {}^4 8_{1/2} \\
 &\quad + {}^2 8_{3/2} + {}^2 8_{1/2} + {}^2 10_{3/2} + {}^2 10_{1/2} + {}^2 1_{3/2} + {}^2 1_{1/2} .
 \end{aligned} \tag{1.32}$$

To describe the angular dependence of the coordinate function, it is convenient to expand it in terms of an orthonormal basis. For the P -wave 70-plet it is natural to consider functions $Y_{1\ell}(\mathbf{n}_{23})$ (P -wave between quarks with coordinates \mathbf{r}_2 and \mathbf{r}_3) and $Y_{1\ell}(\mathbf{r}_{1,23})$ ($\mathbf{n}_{1,23} \sim 2\mathbf{r}_1 - \mathbf{r}_2 - \mathbf{r}_3$, P -wave between quark \mathbf{r}_1 , and the S -wave pair $\mathbf{r}_2, \mathbf{r}_3$). The expansion with respect

to this basis (together with the corresponding spin-flavour functions) gives

$$\begin{aligned}
|{}^4 8_J\rangle_{J_z} &= \frac{1}{\sqrt{2}} \sum_{\ell, \sigma} C_{1\ell \frac{3}{2}\sigma}^{JJ_z} \left\{ |8\rangle_\lambda \left| \frac{3}{2}\sigma \right\rangle Y_{1\ell}(\mathbf{n}_{1,23}) + |8\rangle_\rho \left| \frac{3}{2}\sigma \right\rangle Y_{1\ell}(\mathbf{n}_{23}) \right\} , \\
|{}^2 8_J\rangle_{J_z} &= \frac{1}{\sqrt{2}} \sum_{\ell, \sigma} C_{1\ell \frac{1}{2}\sigma}^{JJ_z} \left\{ \left[-|8\rangle_\lambda \left| \frac{1}{2}\sigma \right\rangle_\lambda + |8\rangle_\rho \left| \frac{1}{2}\sigma \right\rangle_\rho \right] Y_{1\ell}(\mathbf{n}_{1,23}) \right. \\
&\quad \left. + \left[|8\rangle_\lambda \left| \frac{1}{2}\sigma \right\rangle_\rho + |8\rangle_\rho \left| \frac{1}{2}\sigma \right\rangle_\lambda \right] Y_{1\ell}(\mathbf{n}_{23}) \right\} , \quad (1.33) \\
|{}^2 0_J\rangle_{J_z} &= \frac{1}{\sqrt{2}} \sum_{\ell, \sigma} C_{1\ell \frac{1}{2}\sigma}^{JJ_z} \left\{ |10\rangle \left| \frac{1}{2}\sigma \right\rangle_\lambda Y_{1\ell}(\mathbf{n}_{1,23}) + |10\rangle \left| \frac{1}{2}\sigma \right\rangle_\rho Y_{1\ell}(\mathbf{n}_{23}) \right\} , \\
|{}^2 1_J\rangle_{J_z} &= \frac{1}{\sqrt{2}} \sum_{\ell, \sigma} C_{1\ell \frac{1}{2}\sigma}^{JJ_z} \left\{ -|1\rangle \left| \frac{1}{2}\sigma \right\rangle_\rho Y_{1\ell}(\mathbf{n}_{1,23}) + |1\rangle \left| \frac{1}{2}\sigma \right\rangle_\lambda Y_{1\ell}(\mathbf{n}_{23}) \right\} .
\end{aligned}$$

1.3 Estimation of Masses of the Constituent Quarks in the Quark Model

There exists a set of predictions of the quark model, which show clearly and unambiguously that even the simple, naive quark model gives an adequate (though qualitative) description of the hadron structure. We consider these predictions in the present section.

1.3.1 Magnetic moments of baryons

If the constituent quarks can be handled as quasiparticles, they have to be virtually the same in different hadrons. It is convenient to test this by the investigation of the magnetic moments of baryons (this, in fact, was historically the first serious success of the model). For definiteness, let us consider the proton magnetic moment; according to the quark model, it has to be the sum of magnetic moments of the constituent quarks:

$$\frac{e}{2m_p} \mu_p = \sum_{i=1,2,3} \left\langle p_{\frac{1}{2}} \left| \frac{e_q(i) \sigma_Z(i)}{2m_q(i)} \right| p_{\frac{1}{2}} \right\rangle , \quad (1.34)$$

where σ_Z (or σ_3) is the Pauli matrix (see Appendix 1.A). In the framework of the naive quark model we assume $m_u = m_d = m_p/3$, *i.e.* the masses of light non-strange quarks are just one third of the nucleon mass. The matrix element in the right-hand side of (1.34) is determined just by the

spin-flavour part of the proton wave function (it is explicitly given in the previous section). Owing to the normalisation, the coordinate part is unity. The magnetic moment μ_p is expressed in $e/2m_p$ units (*i.e.* in nuclear magnetons). The baryon magnetic momenta calculated this way are given in Table 1.1, where the notation

$$\xi = \frac{m_s - m_u}{m_u}$$

is used. Here $\xi \simeq 1/2$ corresponds to $m_s - m_u \simeq 150$ MeV, which is a rather fundamental quantity for both the quark model and chiral perturbation theory based on QCD [34].

The agreement between calculation and experiment is quite satisfactory (and typical for the naive quark model): the deviations are within 20–25%. However, if one tries to treat these deviations literally, the result will be distressing. For example, calculating the quark masses on the basis of data on μ_{Ξ^0} and μ_{Ξ^-} , one gets $m_u > m_s$. One has to remember that the non-relativistic quark model is a rough approach, and such discrepancies are more or less natural. Small variations of the magnetic moments (in comparison with the calculated values) can be, for instance, consequences of either relativistic corrections, or the structure of the dressed quarks themselves. Introducing, *e.g.* a relatively small anomalous magnetic moment for the u, d and s quarks [35] (see also [36]), one can get a better agreement with the data.

Table 1.1 Magnetic moments of baryons in nuclear magnetons.

Particle	Quark model prediction ($\xi=1/2$)	Experiment
p	3	2.79
n	-2	-1.91
Λ	$-1 + \xi = -0.5$	-0.61
Σ^+	$3 - \frac{1}{3}\xi = 2.84$	2.46
Σ^-	$-1 - \frac{1}{3}\xi = -1.16$	-1.16 ± 0.03
Ξ^0	$-2 + \frac{4}{3}\xi = -1.33$	-1.25 ± 0.01
Ξ^-	$-1 + \frac{4}{3}\xi = -0.33$	-0.65 ± 0.04

1.3.2 Radiative meson decays $V \rightarrow P + \gamma$

The radiative decay of a vector meson V with the production of a pseudoscalar P (reaction $V \rightarrow \gamma P$) is determined by the magnetic moments of

Table 1.2 Values of $\sqrt{\Gamma(V \rightarrow P + \gamma)}$, $\text{keV}^{1/2}$ for vector meson decays.

Decay mode	$\sqrt{\Gamma(V \rightarrow P + \gamma)}$, $\text{keV}^{1/2}$	
	Quark model prediction	Experiment
$\omega \rightarrow \pi^0 \gamma$	34.6	26.9 ± 0.9
$\rho^- \rightarrow \pi^- \gamma$	11.0	8.2 ± 0.4
$\rho^0 \rightarrow \eta \gamma$	8.4	8.1 ± 0.9
$\phi \rightarrow \eta \gamma$	10.4	7.6 ± 0.1
$K^{*\pm} \rightarrow K^- \gamma$	7.0	7.1 ± 0.3
$K^{*0} \rightarrow K^0 \gamma$	13.7	10.8 ± 0.5

the constituent quarks:

$$A_{V \rightarrow \gamma P} \sim \sum_{i=q, \bar{q}} \left\langle V \left| \frac{e_i \sigma_Z(i)}{2m_i} \right| P \right\rangle. \quad (1.35)$$

These processes are transitions of the type of $\omega \rightarrow \gamma \pi^0$, $\phi \rightarrow \gamma \eta$, *etc.* If the idea of the constituent quarks is correct, these transitions must be determined by the same quark masses (and, respectively, magnetic moments), which gave us the magnetic moments of the baryons.

In Table 1.2 we present the calculated values and the experimental data. We use here $\sqrt{\Gamma(V \rightarrow P + \gamma)}$, since this quantity is proportional to the quark magnetic moment, and is, therefore, suitable for comparison with the calculated magnetic moment. The predictions for the radiative widths satisfy the experimental data within the same accuracy of 20–25%. It is a rather impressive fact that the quark magnetic moments are the same in mesons and baryons; this shows that the dressed quarks appear in hadrons as somewhat independent objects — quasiparticles.

In Chapters 6 and 7 we give a detailed discussion of radiative decays in the framework of the quark model.

1.3.3 Empirical mass formulae

It was understood already relatively long ago [37] that the mass splitting of light hadrons can be well described in the framework of the non-relativistic quark model by the spin–spin quark interaction. The next step was made by de Rújula, Georgi and Glashow: according to [38], the hadron mass splitting is due only to the short-range part (the spin–spin part) of the interaction, which is connected to the gluon exchange. The obtained effective potential for the interaction of two quarks (i and j) is supposed to be

$$V_{ij} = \pm \alpha_s \left(\frac{\lambda(i)}{2} \frac{\lambda(j)}{2} \right) \left(-\frac{2\pi}{3} \cdot \frac{\sigma(i)\sigma(j)}{m_q(i)m_q(j)} \delta(\mathbf{r}_{ij}) \right), \quad (1.36)$$

where α_s is the gluon–quark coupling constant squared, λ are the Gell-Mann matrices (see Appendix 1.A), acting on the colour indices of the i th and j th quarks, and the signs \pm stand for the interactions of two quarks or a quark and an antiquark, respectively. It is assumed that the remaining part of the interaction, which is due to the gluon exchange, is averaged, and gives a contribution to the potential which confines the quarks. The interaction (1.36) leads in Born approximation to the following mass splitting:

$$\Delta M_{meson} = \frac{8\pi}{9} \alpha_s |\Psi_M(0)|^2 \left\langle h_M \left| \frac{\sigma(1)\sigma(2)}{m_q(1)m_q(2)} \right| h_M \right\rangle, \quad (1.37)$$

$$\Delta M_{baryon} = \frac{4\pi}{9} \alpha_s \sum_{i \neq j} \int d^3 r_k |\Psi_B(\mathbf{r}_{ij} = 0, \mathbf{r}_k)|^2 \left\langle h_B \left| \frac{\sigma(i)\sigma(j)}{m_q(i)m_q(j)} \right| h_B \right\rangle.$$

The spin–flavour part of matrix elements is calculated exactly; however, in such an approach it is impossible to define the coordinate part of the wave function. Because of that, the expressions $\alpha_s |\Phi_M(0)|^2$ and $\alpha_s \int d^3 r_k |\Phi_B(0, \mathbf{r}_k)|^2$ should be considered as phenomenological constants, which can be obtained from the comparison of masses in the meson and baryon multiplets. The result of the comparison of formulae (1.37) with experiment is demonstrated in Table 1.3. Note that in the calculations we take $|\Phi_M(0)|^2 = \int d^3 r |\Phi_B(0, \mathbf{r})|^2$. This also shows that it is roughly equiprobable to find two quarks or a quark–antiquark pair on a relatively small distance in a hadron. The relations (1.37) are valid also in the case of charmed particles (D and D^* are states of $c\bar{q}$, where $q = u, d$, with $J^P = 1^-$ and 0^- ; D_s^* and D_s — states of $c\bar{s}$ with $J^P = 1^-$ and 0^-). The constant $\alpha_s |\Phi_M(0)|^2$ is the same as for light hadrons (see Table 1.3).

Table 1.3 Baryon mass splitting values calculated in the model of de Rújula–Georgi–Glashow. It is assumed that $m_u = m_d = 360$ MeV, $m_s/m_u = 3/2$, $m_c = 1440$ MeV, $|\Phi_M(0)|^2 = \int d^3 r |\Phi_B(0, \mathbf{r})|^2$.

ΔM	Calculated (MeV)	Exp. (MeV)	ΔM	Calculated (MeV)	Exp. (MeV)
$m_\Delta - m_N$	300	295	$m_\rho - m_\pi$	600	630
$m_\Sigma - m_\Lambda$	68	77	$m_{K^*} - m_K$	400	398
$m_{\Sigma^*} - m_\Lambda$	267	274	$m_{D^*} - m_D$	150	140
$m_{\Xi^*} - m_\Xi$	200	217	$m_{D_s^*} - m_{D_s}$	100	120

The de Rújula–Georgi–Glashow approach allows us to understand and write an explicit expression for baryon masses on a rather elementary level of the quark model. This possibility was discussed in [39], where, for the

masses of the S-wave 56-plet baryons, the expression

$$m_B = \sum_i m_q(i) + b \sum_{i \neq k} \frac{\sigma(i)\sigma(j)}{m_q(i)m_q(j)} \quad (1.38)$$

was suggested. The phenomenological parameter was found from the experiment, and there is an astonishingly good description of the baryon masses (see Table 1.4). The discrepancies between predictions and mea-

Table 1.4 Baryon masses calculated in terms of Eqs. (1.38, 1.39).

	mass (MeV)			mass (MeV)	
Baryon	Prediction	Exp.	Baryon	Prediction	Exp.
N	930	937	Σ^*	1377	1384
Δ	1230	1232	Ξ	1329	1318
Σ	1178	1193	Ξ^*	1529	1533
Λ	1110	1116	Ω	1675	1672

sured data are about 5–6 MeV. However, in trying to write a similar formula for mesons, one fails: the systematic deviations between calculation and experiment are of the order of 100 MeV (the calculated mass values for the ρ and π mesons are $m_\rho = 875$ MeV, $m_\pi = 275$ MeV). The reason for this discrepancy becomes obvious when one calculates the average quark mass in a meson and in a baryon:

$$\begin{aligned} \langle m_q \rangle_M &= \frac{1}{2} \left(\frac{1}{4} m_\pi + \frac{3}{4} m_\rho \right) = 303 \text{ MeV} , \\ \langle m_q \rangle_B &= \frac{1}{3} \left(\frac{1}{2} m_N + \frac{1}{2} m_\Delta \right) = 363 \text{ MeV} . \end{aligned} \quad (1.39)$$

In these combinations of hadron masses, the contribution of the splitting interaction (1.37) cancels completely. Equation (1.39) tells us that the quark masses in mesons are “eaten” by some additional interactions.

1.4 Light Quarks and Highly Excited Hadrons

We saw that low mass hadrons can be considered, in a way, similar to light nuclei (if we substitute nucleons by constituent quarks). The highly excited hadrons open before us, however, a new and intriguing world.

In the last two decades the highly excited states were intensely studied experimentally. Not aiming at completeness, we mention here a list of experiments, partial wave analyses and collaborations and groups: PNPI-RAL [40, 41, 42], PNPI [43, 44, 45], WA102 [46], GAMS [47, 48, 49], VES

[50], Crystal Barrel [51, 52]. They gave us a lot of information for the reanalysis of our notion of the quark–gluon structure of hadrons.

1.4.1 *Hadron systematisation*

The analysis of the Crystal Barrel experiments given by the PNPI–RAL group [42] leads to the discovery of a large number of meson resonances in the mass region 1950 – 2450 MeV. This resulted in the systematisation of $q\bar{q}$ states on the (n, M^2) planes (where n is the radial quantum number of a meson with mass M). As it turned out, mesons with the same J^{PC} but different n fit well to the linear trajectories [53]:

$$M^2(J^{PC}) = M_0^2(J^{PC}) + \mu^2(n - 1). \quad (1.40)$$

Here $M_0(J^{PC})$ is the mass of the ground state ($n = 1$), while μ^2 is a universal constant $\mu^2 = 1.25 \pm 0.05 \text{ GeV}^2$. Thus it became quite easy to construct trajectories also on the (J, M^2) plane and to build not only the basic trajectories but also a large number of daughter trajectories. This systematisation made it possible to obtain meson nonets for sufficiently high orbital and radial excitations. (All this will be discussed in detail in Chapters 2 and 8.)

The systematisation (1.40) is of great significance, however, not only in this sense. As it turns out, virtually all, sufficiently well established resonances are placed on the linear $q\bar{q}$ trajectory. Thus, there is practically no room for non- $q\bar{q}$ states such as four-quark states, $q\bar{q}q\bar{q}$, and hybrids $q\bar{q}g$. Indeed, copious non- $q\bar{q}$ states should have masses above 1500 MeV (remind that the mass of the effective gluon g is of the order of 700 – 1000 MeV, the masses of the light constituent quarks u and d are about 300 – 350 MeV).

Why in the case of mesons Nature does not "imitate" light nuclei so easily, refusing to produce states consisting of a large number of constituents — in contrast to the case of nuclei? We do not have an answer to this question, but it is definitely very important for understanding the character of forces between coloured objects at large distances.

The construction of baryon trajectories in the (n, M^2) plane exposes one more puzzle. Indeed, these trajectories are in accordance with the linear trajectories of the (1.40) type, with the same $\mu^2 \simeq 1.25 \text{ GeV}^2$ value. Does this mean the universality of forces at large distances, acting between the quark and a two-quark system called diquark?

1.4.2 Diquarks

It is an old idea that a qq -system inside a baryon can be separated as a specific object and the quark interactions can be considered as interactions of a quark with a qq -system $q + (qq)$. Such a hypothesis was used in [54] for the description of hadron–hadron collisions. In [55] baryons were described as quark–diquark systems. In hard processes on nuclei, the coherent qq -state (composite diquark) can be responsible for the interaction in the region of large Bjorken x -values, at $x \sim 2/3$; deep inelastic scatterings were considered in the framework of such an approach in [56]. A more detailed picture of the diquark and its applications can be found in [57, 58, 59].

There are two diquark states which have to be taken into account when considering the baryons, namely: qq -states with an orbital momentum $\ell = 0$, a pseudovector diquark and a scalar diquark:

$$J = 1^+ \quad d_1, \quad J = 0^+ \quad d_0. \quad (1.41)$$

If highly excited baryon states are formed in Nature as states of a quark–diquark system, with two possible types (1.41) of diquarks, the variety of highly excited states is seriously reduced, while the classification of the lowest baryons remains unchanged.

There is one more important consequence of the quark–diquark structure of highly excited states: the radial and angular excitations of the qd and $q\bar{q}$ systems must be similar, since the diquark and the antiquark have the same colour charge.

In the recently considered quark models (*e.g.*, see [60, 61, 62]), the baryon states are described by forces of the same structure in the qq and the $q\bar{q}$ sectors (with the obvious replacement of charges when changing from a quark to an antiquark). The cited works contain different hypotheses about the quark–quark (or quark–antiquark) interactions. Still, all they lead to the same specific result for the spectra: the calculated number of highly excited states turns out to be much larger than that of the observed resonances.

This is quite natural for the three-quark models. Indeed, three-quark systems are characterised by two coordinates: the relative distance \mathbf{r}_{12} between quarks 1 and 2, and the coordinate of the third quark, \mathbf{r}_3 . Accordingly, qqq -states can be determined by two orbital momenta ℓ_{12} and ℓ_3 , and by two radial excitations n_{12} and n_3 . There are also many spin states: $s_{12} = 0, 1$ and $S = |s_{12} + s_3| = 1/2, 1/2, 3/2$. Naturally, this variety is restricted by the imposed requirement of complete antisymmetry, but even

so, the number of remaining states is rather large. And it is just this large number of three-quark states which is not confirmed experimentally.

Experimental data on baryon states are unfortunately scarce compared to meson data. So a possible attitude is to wait and see, not drawing any conclusions before having more baryon data. We can, however, take seriously the information we have so far, as an indication that the number of highly excited baryon states is much smaller than expected. If so, we have to reconsider our view on the character of interactions in the $q\bar{q}$ and qq channels and to take into account that interactions in these channels may be quite different.

1.5 Scalar and Tensor Glueballs

Experimentally, we do not observe many mesons with masses higher than 1500 MeV, which could not be placed on the $q\bar{q}$ trajectories in (n, M^2) planes. This is, from our point of view, the main argument against the existence of exotic $q\bar{q}g$ and $qq\bar{q}\bar{q}$ states. As was mentioned above, if $q\bar{q}g$ and $qq\bar{q}\bar{q}$ states existed, we should observe a large number of highly excited states with both exotic and non-exotic quantum numbers, which, as we saw already, is not the case.

This does not mean, of course, that announcements of the observation of exotic mesons would not appear regularly. The reason is not the absence of sufficiently reliable experiments but rather the lack of really qualified analysis of the data. (Reviews about the search for $q\bar{q}g$, $qq\bar{q}\bar{q}$ and other states, such as, *e.g.*, the pentaquarks, can be found in [63, 64]).

To handle this problem, we devote Chapters 3, 4, 5 and 6 to the technique of investigating experimental spectra in the framework of partial wave analysis. In Chapter 3 we consider the scattering of spinless particles, and elements of the K-matrix technique and of the dispersion N/D method are presented. In Chapter 4 collisions of fermions, NN and $N\bar{N}$, are described; expressions for the amplitudes of the production of large spin particles are given. Chapter 5 is devoted to πN and γN collisions.

The analysis of mesonic spectra allowed us to discover two broad isoscalar states in the channels $J^{PC} = 0^{++}$ (see Chapter 3) and $J^{PC} = 2^{++}$ (Chapter 4).

- (i) They are superfluous from the point of view of the (n, M^2) systematisation;

- (ii) the constants of their decays into pseudoscalar mesons satisfy relations corresponding to glueballs; the decays are nearly flavour blind.

The masses and widths of these glueballs are as follows.

Scalar glueball [65, 66, 67, 68, 69, 70]:

$$0^{++} - \text{glueball} : \quad M \simeq 1200 - 1600 \text{ MeV} \quad \Gamma \simeq 500 - 900 \text{ MeV} , \quad (1.42)$$

tensor glueball [76, 74, 75]:

$$2^{++} - \text{glueball} : \quad M = 2000 \pm 30 \text{ MeV}, \quad \Gamma = 500 \pm 50 \text{ MeV}. \quad (1.43)$$

The status of the tensor glueball is rather well defined: it was seen in several experiments [71, 72, 73], and the decay couplings tell us that $f_2(2000)$ is nearly flavour blind [74, 75]. Besides, the $f_2(2000)$ is an extra state in (n, M^2) trajectories [76].

More ambiguous is the existence of the scalar glueball: its mass and width are determined with large errors. However, the ratios of the couplings of the $f_0(1200 - 1600)$ decays into different channels of two pseudoscalar particles, $f_0(1200 - 1600) \rightarrow \pi\pi, K\bar{K}, \eta\eta, \eta\eta'$ are comparatively well defined. These couplings show us that $f_0(1200 - 1600)$ is very close to a flavour singlet (so this state is flavour blind with a good accuracy). Moreover, from the point of view of the $q\bar{q}$ -systematics this state turned out to be superfluous (see Chapter 2). Hence, it is natural to identify it with a scalar glueball.

The mass $f_0(1200 - 1600)$ is twice the mass of the soft effective gluon ($m_g \simeq 700 - 1000 \text{ MeV}$), so, seemingly, this state could be considered also as a gluonium, gg . Still, this would be a rather conditional notation for $f_0(1200 - 1600)$. Indeed, it was produced as a result of a strong mixing with its neighbouring resonances: the evidence for that is both the large width of the resonance and the fact that the gluonium mixes easily with $q\bar{q}$ states (the latter will be discussed in Chapter 2). So it is reasonable to call the $f_0(1200 - 1600)$ state a gluonium descendant. In fact, its wave function is a Fock column

$$f_0(1200 - 1600) = \begin{pmatrix} gg \\ q\bar{q} \\ \pi\pi, K\bar{K}, \eta\eta, \eta\eta' \\ \pi\pi\pi\pi \\ qq\bar{q}\bar{q} \\ \dots \end{pmatrix} \quad (1.44)$$

and it is not certain at all that the gluonium component gg strongly dominates. Thus, to follow the tradition, we call $f_0(1200 - 1600)$ (though rather

conditionally) a glueball, having in mind that it is, probably, a mixture of states of the type shown in (1.44).

Similarly, the tensor glueball $f_2(2000)$ is a mixture of different states. In this case, however, the components with vector particles may be significant as well:

$$f_2(2000) = \begin{pmatrix} gg \\ q\bar{q} \\ \pi\pi, K\bar{K}, \eta\eta, \eta\eta' \\ \rho\rho, \omega\omega, \phi\phi, \omega\phi \\ \dots \end{pmatrix}. \quad (1.45)$$

The tensor glueball lies on the pomeron trajectory

$$\alpha_{\mathbf{P}}(M^2) = \alpha_{\mathbf{P}}(0) + \alpha'_{\mathbf{P}}(0)M^2, \quad (1.46)$$

where $\alpha_{\mathbf{P}}(0) \simeq 1.1 - 1.3$, $\alpha'_{\mathbf{P}} \simeq 0.15 - 0.25 \text{ GeV}^{-2}$. The scalar glueball has to be placed on a daughter trajectory. Assuming that the daughter trajectory is also linear and is characterized by the same slope as the basic trajectory, we have

$$\alpha_{\mathbf{P}(\text{daughter})}(M^2) = \alpha_{\mathbf{P}(\text{daughter})}(0) + \alpha'_{\mathbf{P}}(0)M^2; \quad (1.47)$$

here $\alpha_{\mathbf{P}(\text{daughter})}(0) \simeq -0.5$. This means that the next tensor state lying on this trajectory must be near 3500 MeV (see Fig. 1.2).

The scalar glueball was detected as a result of a set of subsequent K-matrix analyses [66, 67, 68, 69, 70]. In the course of these investigations the energy (or the invariant mass) of $\pi\pi$ was successively increased and more and more channels ($K\bar{K}$, $\eta\eta$, $\eta\eta'$, $\pi\pi\pi\pi$) were included. In the beginning, when the invariant mass of the considered spectra was small ($\sqrt{s} < 1500$ MeV [66, 67]), the status of the broad resonance was questionable, since its mass was on the verge of the spectra. In the subsequent investigations [68, 69] the mass interval was increased up to 2000 MeV, and the position of the broad resonance was stabilised in the region of 1400 MeV (although with a large error, of the order of ± 200 MeV). There is an essential difference between the quark contents of the scalar and the tensor resonances. The scalar resonances are the mixtures of non-strange ($n\bar{n} = (u\bar{u} + d\bar{d})/\sqrt{2}$) and strange ($s\bar{s}$) quarkonia, while the tensor resonances are either dominant $n\bar{n}$ -states, or the $s\bar{s}$ is dominating. We have to remember that, while the $q\bar{q}$ component may be large in a glueball, the gluonium component cannot be large in a $q\bar{q}$ state owing to the fact that gg is smeared over a number of neighbouring states.

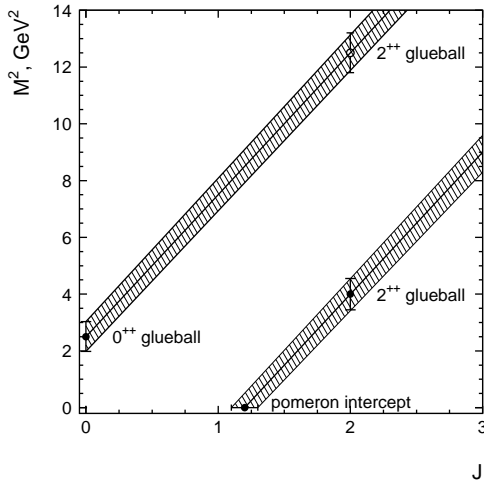


Fig. 1.2 Glueball states on the pomeron trajectories (full circles) and the predicted second tensor glueball (open circle).

The $f_0(450)$ called the σ -meson is a particular state. Strictly speaking, we are not sure that the σ -meson exists at all. However, if it exists, it could be a rather remarkable particle: the visible "remnant" of the white component of the scalar confinement forces.

1.5.1 Low-lying σ -meson

The K -matrix analysis of the $(0, 0^{++})$ wave does not give a definite answer to the question whether the σ -meson exists. Indeed, the applicability of the K -matrix analysis is restricted in the small \sqrt{s} region, since the K -matrix amplitude cannot give an adequate description of the left cut of the partial amplitude at $s \leq 0$. In [77], the analysis of the $\pi\pi$ amplitude at $280 \leq \sqrt{s} \leq 900$ MeV was carried out in the framework of the dispersion N/D method. Performing the N/D -fit, we have used there, on the one hand, experimental data on the scattering phase in the region 280–500 MeV, and, on the other hand, the K -matrix amplitude [69] in the 450–900 MeV region. As a result, we got a resonance pole near the $\pi\pi$ threshold denoted as $f_0(450)$ (see Chapter 2 for more detail).

The light σ -meson is a possible manifestation a component (the white one) of the singular colour forces responsible for confinement. The scalar confinement potential describing the $q\bar{q}$ state spectrum in the 1500 - 2500

MeV region behaves at large hadron distances as $V(r) \sim r$, in the momentum representation this leads to a $1/q^2$ -type singularity in the $q\bar{q}$ amplitude. In the white channel, the transition

$$\textit{white singular term} \longrightarrow \pi\pi \longrightarrow \textit{white singular term} \quad (1.48)$$

exists, owing to which the singularities of the white amplitude may occur on the second (unphysical) sheet of the complex- s plane. It is just this singular term which may turn out to be the object we call σ . This scenario is considered in more detail in Chapter 3, where the scalar and tensor states are discussed.

1.6 High Energies: The Manifestation of the Two- and Three-Quark Structure of Low-Lying Mesons and Baryons

We have seen (Sections 1.4.1 and 1.4.2) that the investigation of highly excited hadrons may raise a doubt in the correctness of our picture of strongly interacting quarks and gluons. There could be a challenge to act as was suggested by I.Ya. Pomeranchuk: "erase everything, let us start again". Still, the physics of high-energy collisions of low-lying hadrons (pions, kaons, nucleons) prevent us from rushing to such a conclusion. Indeed, experimental data collected in the field of high energy collisions in the last five decades show unambiguously that low-lying mesons (π , K) and baryons consist of two and three constituent quarks, respectively.

We shall recall here some of the most striking and important facts. For a detailed description, see [78].

1.6.1 Ratios of total cross sections in nucleon–nucleon and pion–nucleon collisions

At moderately high energies, at momenta $p_{lab} \sim 5 - 300$ GeV/c of the incoming particles, the ratio of the total cross sections can be described by

$$\sigma_{tot}(NN)/\sigma_{tot}(\pi N) = 3/2 \quad (1.49)$$

with quite a good accuracy (of the order of 10%).

This ratio was initiated by V.N. Gribov and I.Ya. Pomeranchuk. Later on it was considered in many papers [79, 80]. The additive quark model is based just on this relation: if the constituent quarks are separated in space,

the main process is the collision of a quark of the incident hadron with a quark of the target hadron (see Fig. 1.3).

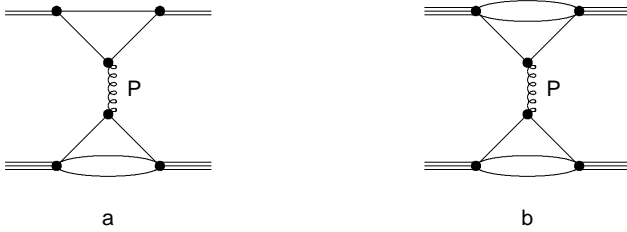


Fig. 1.3 Pion–nucleon and nucleon–nucleon scattering in the constituent quark model with pomeron exchange.

There are six meson–nucleon collisions and nine nucleon–nucleon collisions of this type. Since the total cross sections $\sigma_{tot}(NN)$ and $\sigma_{tot}(\pi N)$ are proportional to the imaginary parts of the diagrams shown in Fig. 1.3, we obtain the relation (1.49).

1.6.2 Diffraction cone slopes in elastic nucleon–nucleon and pion–nucleon diffraction cross sections

The elastic diffraction cross sections determined by the diagrams Fig. 1.3 read (see [78, 79, 80]):

$$\begin{aligned} \frac{d\sigma}{d|t|}(NN \rightarrow NN) &\sim F_N^4(t) |A_{qq}(t)|^2, \\ \frac{d\sigma}{d|t|}(\pi N \rightarrow \pi N) &\sim F_\pi^2(t) F_N^2(t) |A_{qq}(t)|^2, \end{aligned} \quad (1.50)$$

where $F_\pi(t)$ and $F_N(t)$ are triangle quark blocks, and $A_{qq} \simeq A_{q\bar{q}}$ at high energies.

On the other hand, the charge form factors of the pion $f_\pi(t)$ and of the nucleon $f_p(t)$ are determined by the processes in Fig. 1.4, i.e. by triangle diagrams of the same type as those defining the diffraction cone in (1.50). Hence,

$$f_\pi(t) = F_\pi(t) f_q(t), \quad f_p(t) = F_p(t) f_q(t). \quad (1.51)$$

Here $f_q(t)$ is the form factor of the constituent quark. Since in the model the constituent quarks are supposed to be relatively small objects compared to the hadron size,

$$\langle r_q^2 \rangle \ll \langle R_{hadron}^2 \rangle, \quad (1.52)$$

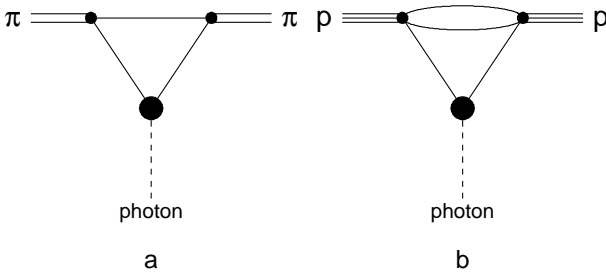


Fig. 1.4 Charge form factors of pion and proton in the additive quark model.

we can, in a rough approximation, neglect the t -dependence in both $f_q(t)$ and $A_{qq}(t)$ (though in the latter at moderately high energies only, when the pomeron size is small). Hence, considering the t -dependence at moderately high energies ($p_{lab} \sim 5 - 100 \text{ GeV}/c$) we can take

$$\frac{d\sigma}{d|t|}(NN \rightarrow NN) \sim F_N^4(t), \quad \frac{d\sigma}{d|t|}(\pi N \rightarrow \pi N) \sim F_\pi^2(t)F_N^2(t), \quad (1.53)$$

where $F_\pi(t)$ and $F_N(t)$ are charge form factors of the pion and the proton. Experimental data on the slopes of diffraction cones are well described by Eq. (1.53).

1.6.3 Multiplicities of secondary hadrons in e^+e^- and hadron-hadron collisions

The multiplicity of the secondary (*i.e.* newly produced) hadrons in e^+e^- collisions is determined by the process shown in Fig. 1.5a: the virtual photon produces a high energy $q\bar{q}$ pair; in their turn the quarks, flying away, give rise to a jet (or comb) of hadrons. Similar processes take place also in hadron-hadron collisions [81], they are shown in Figs. 1.5b (pion-nucleon collision) and 1.5c (nucleon-nucleon collision). In the central region, the multiplicities of the newly produced particles are equal for all these three processes, if only the energies of e^+e^- , $q\bar{q}$ and qq are equal.

Such an equality of the multiplicities is confirmed by experiment (see [78] and references therein).

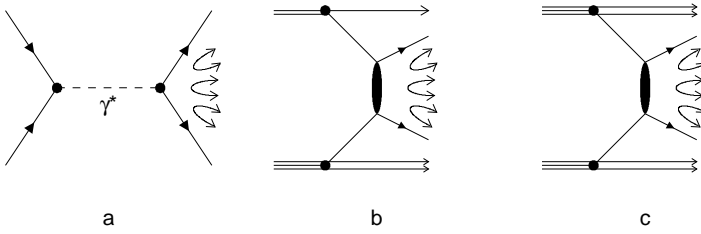


Fig. 1.5 Multiple production of hadrons in e^+e^- collisions and in πN and NN collisions where $qq \rightarrow \text{hadrons}$ and $q\bar{q} \rightarrow \text{hadrons}$ transitions are dominating.

1.6.4 Multiplicities of secondary hadrons in πA and pA collisions

The two quarks of a pion or the three quarks of a nucleon are not able to pass a very heavy nucleus without interacting (see Fig. 1.6). If so, in πA and NA processes the multiplicities have to be related as [82]:

$$\left[\frac{\langle n \rangle_{NA}}{\langle n \rangle_{\pi A}} \right]_{A \rightarrow \infty} = \frac{3}{2}. \quad (1.54)$$

Real nuclei are not massive enough to produce this ratio explicitly. But, on the basis of experimental data, one can write $\langle n_{ch} \rangle_{pA} / \langle n_{ch} \rangle_{\pi A}$ as a function of A . In this case, it can be clearly seen that this relation goes to $3/2$ as A is growing (for details, see [78]).

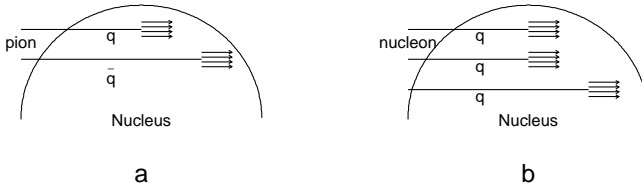


Fig. 1.6 Multiple production of hadrons in πA and NA collisions with heavy nuclei: in this case all quarks of the incoming particles interact with the nuclear matter.

1.6.5 Momentum fraction carried by quarks at moderately high energies

It is obvious from Figs. 1.5b and 1.5c that the colliding quark of the meson carries $\sim 1/2$ of the meson momentum, while the colliding quark of a nucleon carries $\sim 1/3$. These facts have to manifest themselves in the spectra of secondary particles formed by colliding quarks, *i.e.* in the

central region of secondary particle production. Experimental results [83] show that this is, indeed, the case (Fig. 1.7). We see that in the c.m. frame of the colliding hadrons in πp collisions the spectrum of secondary hadrons in the central region is shifted in the direction of the pion motion (Fig. 1.7a). In the centre-of-mass frame of the colliding quarks (Fig. 1.7b), however, the spectrum becomes symmetrical. This proves that the meson consists of two, the baryon of three quarks.

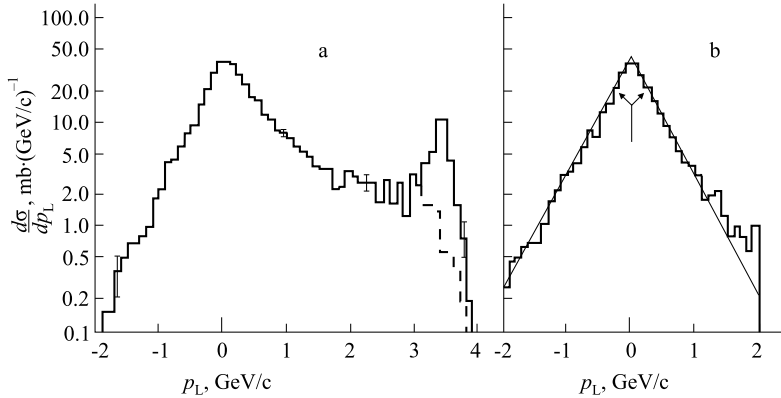


Fig. 1.7 The cross section of the $\pi^- p \rightarrow \pi^\pm$ process at 25 GeV/c in the c.m. system of the colliding particles (a) and in the centre-of-mass frame of the colliding quarks (b). To exclude the effect of the leading particle, the cross section of the $\pi^- p \rightarrow \pi^+$ process (which is close to $\pi^- p \rightarrow \pi^-$ for small x values) is drawn at $p_L > 0$ in Fig. 1.9b. Data are taken from [83].

1.7 Constituent Quarks, QCD-Quarks, QCD-Gluons and the Parton Structure of Hadrons

Attempts to combine the structure of constituent quarks with the results of deep inelastic scatterings were made relatively long ago [84].

1.7.1 Moderately high energies and constituent quarks

The constituent quarks are “dressed quarks” — indeed, from the point of view of the parton picture they consist of QCD-quarks and QCD-gluons. Each of these quark–gluon clusters (*i.e.* constituent quarks) consists of a valence QCD quark (or current quark) surrounded by quark–antiquark pairs and QCD gluons (see Fig. 1.8).

Since the quantum numbers of the constituent quarks and the valence

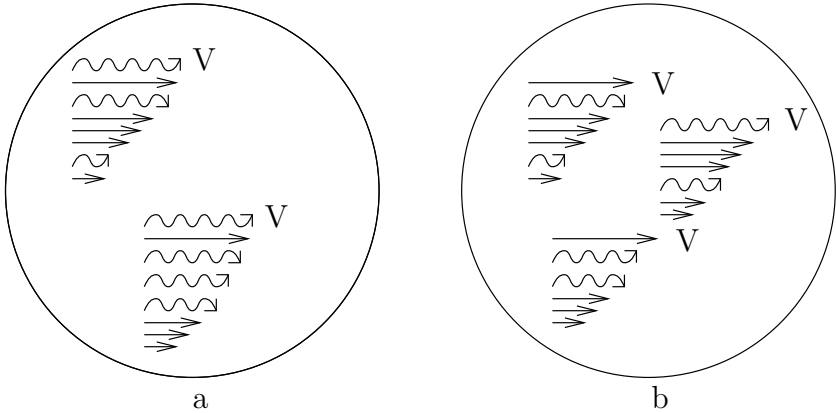


Fig. 1.8 Parton structure of a meson (a) and of a baryon (b). The baryon consists of three (the meson of two) dressed quarks; each dressed quark (antiquark) consists of a valence quark–parton (straight arrow, marked by the index V), sea partons (wavy arrows for gluons and straight arrows for quarks or antiquarks).

quarks coincide, the sea of the quark–antiquark pairs and QCD-gluons is neutral.

Let us note that the picture of spatially separated quarks is true only up to moderately high energies; only then we have three (nucleon) or two (meson) quark–parton clouds (Fig. 1.8). With the growth of energy the transverse dimensions of these clouds increase and we arrive at an essentially new picture of overlapping clouds.

1.7.2 Hadron collisions at superhigh energies

The changes which the clouds of colliding quarks go through while the moderately high energies grow to superhigh ones can be demonstrated in the impact parameter space (see Fig. 1.9).

Figure 1.9a shows the “picture” of a meson, while Fig. 1.9d is that of a nucleon in the impact parameter space (*i.e.* what the incoming hadrons look like from the point of view of the target). In the impact parameter space quarks are black at moderately high energies: this follows from investigations of the proportions of truly inelastic and quasi-inelastic processes [85]. Accordingly, in Figs. 1.9a and 1.9d two (for a meson) and three (for a baryon) black discs are drawn. But, as we just mentioned, the transverse sizes of the discs increase, and at intermediate energies ($p_{lab} \sim 500 - 1000$ GeV/c) the quarks partially overlap (Figs. 1.9b, 1.9e). In this energy region

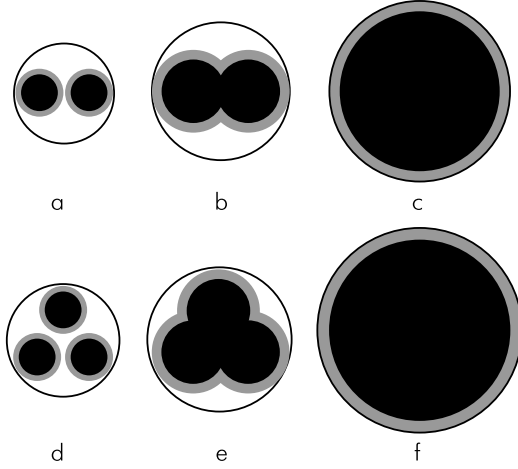


Fig. 1.9 Quark structure of a meson (a–c) and a baryon (d–e) in the constituent quark model. At moderately high energies (a,c) constituent quarks inside the hadron are spatially separated. With the energy increase, quarks become partially overlapped (b,e); at superhigh energies (c,f) quarks are completely overlapped, and hadron–hadron collisions lose the property of additivity.

the additivity may already be broken in the collision processes. Further, there is a total overlap of the clouds (Figs. 1.9c, 1.9f) and, in principle, the meson cross sections cannot be distinguished from the baryon cross sections any more. Indeed, both are just products of the collisions of black discs.

According to estimates given in [86], in this energy region

$$\sigma_{tot}(p\bar{p}) \simeq \sigma_{tot}(\pi p) \simeq 2\sigma_{el}(p\bar{p}) \simeq 2\sigma_{el}(\pi p) \simeq 0.32 \ln^2 s \text{ mb} \quad (1.55)$$

– but this is true only for energies higher than what can be reached at LHC. For energies $0.5 \text{ TeV} \leq \sqrt{s} \leq 20 \text{ TeV}$ the cross sections have to behave as [86]:

$$\begin{aligned} \sigma_{tot}(p\bar{p}) &= 49.80 + 8.16 \ln \frac{s}{9s_0} + 0.32 \ln^2 \frac{s}{9s_0}, \\ \sigma_{tot}(\pi p) &= 30.31 + 5.70 \ln \frac{s}{6s_0} + 0.32 \ln^2 \frac{s}{6s_0}. \end{aligned} \quad (1.56)$$

In (1.56) the numerical coefficients are given in mb, and $s_0 = 10^4 \text{ GeV}^2$. In the region of LHC energies ($\sqrt{s} = 16 \text{ TeV}$) we have

$$\sigma_{tot}(p\bar{p}) = 131 \text{ mb}, \quad \sigma_{el}(p\bar{p}) = 41 \text{ mb}. \quad (1.57)$$

As we see, at LHC energies the asymptotic value $\sigma_{tot} \simeq 1/2\sigma_{el}$ is not reached yet. However, already at these energies another consequence of the

quark overlap reveals itself: the scaling of proton spectra in the fragmentation region is broken at $x = p/p_{max} \sim 2/3$. The spectra of the protons have to decrease sharply in this region [87].

* * *

As was seen above, the hypothesis of hadrons being composite systems of two (mesons) or three (low-lying baryons) constituent quarks works well. But it is a question whether this hypothesis works for highly excited states, namely, whether certain highly excited states consist of a larger number of constituent quarks or contain effective gluons — this question should be answered by further experimental investigations. To avoid misleading conclusions, we should deal with advanced and refined methods for fixing pole singularities of the amplitudes.

Our further presentation is devoted mainly to the techniques used for the study of analytical structure of the amplitudes in hadron collisions.

1.8 Appendix 1.A: Metrics and $SU(N)$ Groups

There are different ways of writing the four-dimensional metric tensor, the γ -matrices, the amplitudes, *etc.*; we present here our choice for them. In addition, we give some useful relations for reference.

1.8.1 Metrics

We use the metric tensor

$$g_{\mu\nu} = \text{diag}(1, -1, -1, -1). \quad (1.58)$$

We do not distinguish between covariant and contravariant vectors, and adopt the notation

$$A_\mu B_\mu = A_0 B_0 - A_1 B_1 - A_2 B_2 - A_3 B_3. \quad (1.59)$$

Summation over doubled subscripts is assumed wherever the opposite is not specified.

1.8.2 $SU(N)$ groups

The fundamental representation space for an $SU(N)$ group is formed by N -component spinors Ψ (columns of N complex numbers or field operators). The transformation

$$\Psi \rightarrow \Psi' = S\Psi \quad (1.60)$$

of the fundamental representation is carried out by $N \times N$ complex matrices which satisfy the unitarity and unimodularity conditions

$$SS^+ = \mathbf{I}, \quad \det S = 1. \quad (1.61)$$

Every matrix S has $N^2 - 1$ real independent parameters ω_a ($a = 1, 2, \dots, N^2 - 1$) and can be represented in the form

$$S = \exp(i\omega_a t_a), \quad (1.62)$$

where $\mathbf{t} = (t_1, t_2, \dots, t_{N^2-1})$ is a fixed set of $(N^2 - 1)$ $N \times N$ matrices. According to (1.61), t_a are Hermitian and traceless:

$$t_a^+ = t_a, \quad \text{Sp}(t_a) = 0. \quad (1.63)$$

Here the matrices t_a are generators of the fundamental representation of the $SU(N)$ group. They are normalised according to the condition

$$\text{Sp}(t_a t_b) = \frac{1}{2} \delta_{ab}. \quad (1.64)$$

Every traceless Hermitian $N \times N$ matrix can be presented as a linear superposition of t_a . The commutator of two t_a matrices is a traceless anti-Hermitian matrix; thus

$$[t_a, t_b] = i f_{abc} t_c. \quad (1.65)$$

The structure constants f_{abc} are real and completely antisymmetric. The matrices \mathbf{t} satisfy the Fierz identities

$$\begin{aligned} \mathbf{I}_{\alpha\beta} \mathbf{I}_{\gamma\delta} &= \frac{1}{N} \mathbf{I}_{\alpha\delta} \mathbf{I}_{\gamma\beta} + 2 \mathbf{t}_{\alpha\delta} \mathbf{t}_{\gamma\beta}, \\ \mathbf{t}_{\alpha\beta} \mathbf{t}_{\gamma\delta} &= \left(\frac{1}{2} - \frac{1}{2} N^2 \right) \mathbf{I}_{\alpha\delta} \mathbf{I}_{\gamma\beta} - \frac{1}{N} \mathbf{t}_{\alpha\delta} \mathbf{t}_{\gamma\beta}, \end{aligned} \quad (1.66)$$

where $\mathbf{I}_{\alpha\beta}$ is a unit $N \times N$ matrix. Below, we present the generators t_a and the structure constants f_{abc} for the simplest groups explicitly.

SU(2)-group:

$$\mathbf{t} = \frac{1}{2} \boldsymbol{\sigma}, \quad (1.67)$$

where $\boldsymbol{\sigma}$ are the Pauli matrices

$$\sigma_1 = \begin{pmatrix} 0 & 1 \\ 1 & 0 \end{pmatrix}, \quad \sigma_2 = \begin{pmatrix} 0 & -i \\ i & 0 \end{pmatrix}, \quad \sigma_3 = \begin{pmatrix} 1 & 0 \\ 0 & -1 \end{pmatrix}. \quad (1.68)$$

The structure constants form a completely antisymmetric unit tensor ε_{abc} :

$$f_{abc} = \varepsilon_{abc}, \quad \varepsilon_{123} = 1. \quad (1.69)$$

$SU(3)$ -group:

$$\mathbf{t} = \frac{1}{2}\boldsymbol{\lambda}, \quad (1.70)$$

where $\boldsymbol{\lambda}$'s are the Gell-Mann matrices

$$\begin{aligned} \lambda_1 &= \begin{pmatrix} 0 & 1 & 0 \\ 1 & 0 & 0 \\ 0 & 0 & 0 \end{pmatrix}, & \lambda_2 &= \begin{pmatrix} 0 & -i & 0 \\ i & 0 & 0 \\ 0 & 0 & 0 \end{pmatrix}, & \lambda_3 &= \begin{pmatrix} 1 & 0 & 0 \\ 0 & -1 & 0 \\ 0 & 0 & 0 \end{pmatrix} \\ \lambda_4 &= \begin{pmatrix} 0 & 0 & 1 \\ 0 & 0 & 0 \\ 1 & 0 & 0 \end{pmatrix}, & \lambda_5 &= \begin{pmatrix} 0 & 0 & -i \\ 0 & 0 & 0 \\ i & 0 & 0 \end{pmatrix}, & \lambda_6 &= \begin{pmatrix} 0 & 0 & 0 \\ 0 & 0 & 1 \\ 0 & 1 & 0 \end{pmatrix} \\ \lambda_7 &= \begin{pmatrix} 0 & 0 & 0 \\ 0 & 0 & -i \\ 0 & i & 0 \end{pmatrix}, & \lambda_8 &= \frac{1}{\sqrt{3}} \begin{pmatrix} 1 & 0 & 0 \\ 0 & 1 & 0 \\ 0 & 0 & -2 \end{pmatrix}. \end{aligned} \quad (1.71)$$

The independent non-zero coefficients f_{abc} are

$$\begin{aligned} f_{123} &= 1, & f_{458} &= f_{678} = \sqrt{3}/2, \\ f_{147} &= f_{516} = f_{246} = f_{257} = f_{345} = f_{637} = 1/2. \end{aligned} \quad (1.72)$$

References

- [1] M. Gell-Mann, Acta Phys. Austriaca (Schladming Lectures) Suppl. IX, 773 (1972).
- [2] M. Gell-Mann, Oppenheimer Lectures, Preprint IAS, Princeton (1975).
- [3] J.D. Bjorken and E. Paschos, Phys. Rev. **186**, 1975 (1969).
- [4] R.Feynman, *Photon-Hadron Interactions*. W.A.Benjamin, New York (1972).
- [5] V.N.Gribov. *Space-Time Description of the Hadron Interactions at High Energies*, Proceedings of the VIIIth LNPI Winter School, (1973); e-Print Archive hep-ph/006158 (2000). Also in V.N. Gribov, *Gauge Theories and Quark Confinement*, Phasis, Moscow (2002)
- [6] T.N. Yang and R.L. Mills, Phys. Rev. **96**, 191 (1954).
- [7] I.B. Khriplovich, Yad. Fiz. **10**, 409 (1969) [Sov. J. Nucl. Phys. **10**, 235 (1970)].
- [8] H.D. Politzer, Phys. Rev. Lett. **30**, 1346 (1973).
- [9] D.J. Gross and F. Wilczek, Phys. Rev. Lett. **30**, 1343 (1973).
- [10] L.D. Faddeev and V.N. Popov, Phys. Lett. **B25**, 29 (1967); *Methods in Field Theory*, Eds. R. Balian and J. Zinn-Justin, North-Holland / World Scientific (1981) and references therein.

- [11] Yu.L. Dokshitzer, D.I. Dyakonov, and S.I. Troyan, *Phys. Rep.* **58C**, 269 (1980).
- [12] K. Huang, *Quarks, Leptons and Gauge Fields*. World Scientific, Singapore (1983).
- [13] K. Moriyasu, *An Elementary Primer for Gauge Theory*. World Scientific, Singapore (1983).
- [14] R.D. Field, *Application of Perturbative QCD*. Frontières in Physics (1989).
- [15] Yu.L. Dokshitzer, V.A. Khoze, A.H. Mueller, and S.I. Troyan, *Basics of Perturbative QCD*. Editions Frontières (1991).
- [16] R.E. Ellis, W.J. Stirling, and B. Webber, *QCD and Collider Physics*, Cambridge University Press (1996).
- [17] E. Fermi and C.N. Yang, *Phys. Rev.* **76**, 1739 (1949).
- [18] S. Sakata, *Prog. Theor. Phys.* **16**, 686 (1956).
- [19] L.B. Okun, *Weak Interactions of Elementary Particles*, State Publishing House for physics and mathematics, Moscow (1963) (in Russian).
- [20] M. Gell-Mann, *Phys. Lett.* **8**, 214 (1964).
- [21] G. Zweig, *An $SU(3)$ Model of Strong Interaction Symmetry and its Breaking*, CERN Rept. No. 8182/TH401 (1964).
- [22] M. Gell-Mann, *The eightfold way*, W.A. Benjamin, NY (1961).
- [23] Y. Ne'eman, *Nucl. Phys.* **26**, 222 (1961).
- [24] Every even year issue of the Review of Particle Physics, *e.g.* W.-M. Jao, *et al.* *J. Phys. G: Nucl. Part. Phys.* **33**, 1 (2006).
- [25] O.W. Greenberg, *Phys. Rev. Lett* **13**, 598 (1964).
- [26] N.N. Bogoliubov, B.V. Struminski, and A.N. Tavkhelidze, Preprint JINR D-1968 (1964).
- [27] M. Han and Y. Nambu, *Phys. Rev.* **B139**, 1006 (1965).
- [28] F. Gürsey and L. Radicati, *Phys. Rev. Lett.* **13**, 173 (1964).
- [29] B. Sakita, *Phys. Rev. B* **136**, 1756 (1964).
- [30] E. Wigner, *Phys. Rev.* **51**, 106 (1937).
- [31] R. Gatto, *Phys. Lett.* **17**, 124 (1965).
- [32] Ya.I. Azimov, V.V. Anisovich, A.A. Anselm, G.S. Danilov, and I.T. Dyatlov, *Pis'ma ZhETF* **2**, 109 (1965) [*JETP Letters* **2**, 68 (1965)].
- [33] R.R. Horgan and R.H. Dalitz, *Nucl. Phys. B* **66**, 135 (1973); R.R. Horgan, *Nucl. Phys. B* **71**, 514 (1974).
- [34] J. Gasser and H. Leutwyler, *Phys. Rep. C* **87**, 77 (1982).
- [35] I.G. Aznauryan and N. Ter-Isaakyan, *Yad. Fiz.* **31**, 1680 (1980) [*Sov. J. Nucl. Phys.* **31**, 871 (1980)].
- [36] S.B. Gerasimov, ArXiv: hep-ph/0208049 (2002).

- [37] Ya. B. Zeldovich and A.D. Sakharov, *Yad. Fiz.* **4**, 395 (1966); [*Sov. J. Nucl. Phys.* **4**, 283 (1967)].
- [38] A. de Rújula, H. Georgi, and S.L. Glashow, *Phys. Rev. D* **12**, 147 (1975).
- [39] S.L. Glashow, *Particle Physics Far from High Energy Frontier*, Harvard Preprint, HUPT-80/A089 (1980).
- [40] V.V. Anisovich, D.V. Bugg, and B.S. Zou, *Phys. Rev. D* **50**, 1972 (1994).
- [41] V.V. Anisovich, D.V. Bugg, and A.V. Sarantsev, *Yad. Fiz.* **62**, 1322 (1999) [*Phys. Atom. Nuclei* **62**, 1247 (1999)].
- [42] A.V. Anisovich, C.A. Baker, C.J. Batty, *et al.*, *Phys. Lett. B* **449**, 114 (1999); **452**, 173 (1999); **452**, 180 (1999); **452**, 187 (1999); **472**, 168 (2000); **476**, 15 (2000); **477**, 19 (2000); **491**, 40 (2000); **491**, 47 (2000); **496**, 145 (2000); **507**, 23 (2001); **508**, 6 (2001); **513**, 281 (2001); **517**, 261 (2001); **517**, 273 (2001); *Nucl. Phys. A* **651**, 253 (1999); **662**, 319 (2000); **662**, 344 (2000).
- [43] A.V. Anisovich, V.V. Anisovich, and A.V. Sarantsev, *Zeit. Phys. A* **359**, 173 (1997).
- [44] A.V. Anisovich, V.V. Anisovich, and A.V. Sarantsev, *Yad. Fiz.* **60**, 2065 (1997).
- [45] V.V. Anisovich and A.V. Sarantsev, *Eur. Phys. J. A* **16**, 229 (2003).
- [46] D. Barberis, *et al.*, (WA 102 Collaboration), *Phys. Lett. B* **453**, 305 (1999); **453**, 316 (1999); **453**, 325 (1999); **462**, 462 (1999); **471**, 429 (1999); **471**, 440 (2000); **474**, 423 (2000); **479**, 59 (2000); **484**, 198 (2000); **488**, 225 (2000).
- [47] D.M. Alde, *et al.*, *Phys. Lett. B* **397**, 350 (1997); *Phys. Atom. Nucl.* **60**, 386 (1997); **62**, 421 (1999).
- [48] D.M. Alde, *et al.*, *Phys. Lett. B* **205**, 397 (1988); Y.D. Prokoshkin and S.A. Sadovsky, *Yad. Phys.* **58**, 662 (1995) [*Phys. Atom. Nucl.* **58**, 606 (1995)]; *Yad. Phys.* **58**, 921 (1995) [*Phys. Atom. Nucl.* **58**, 853 (1995)].
- [49] V.V. Anisovich, A.A. Kondashov, Yu.D. Prokoshkin, S.A. Sadovsky, and A.V. Sarantsev, *Yad. Fiz.* **60**, 1489 (2000) [*Phys. Atom. Nuclei* **60**, 1410 (2000)].
- [50] D.V. Amelin, *at al.*, *Phys. Lett. B* **356**, 595 (1995); *Phys. Atom. Nucl.* **62**, 445 (1999); **67** 1408 (2004); **69**, 690 (2006); *Z. Phys. C* **70**, 70 (1996).
- [51] V.V. Anisovich, D.S. Armstrong, I. Augustin, *et al.* *Phys. Lett. B* **323** 233 (1994).

- [52] C. Amsler, V.V. Anisovich, D.S. Armstrong, *et al.* Phys. Lett. B **333**, 277 (1994).
- [53] A.V. Anisovich, V.V. Anisovich, and A.V. Sarantsev, Phys. Rev. D **62**:051502 (2000).
- [54] V.V. Anisovich, Pis'ma ZhETF **2**, 439 (1965) [JETP Lett. **2**, 272 (1965)].
- [55] M. Ida and R. Kobayashi, Progr. Theor. Phys. **36**, 846 (1966); D.B Lichtenberg and L.J. Tassie, Phys. Rev. **155**, 1601 (1967); S. Ono, Progr. Theor. Phys. **48** 964 (1972).
- [56] V.V. Anisovich, Pis'ma ZhETF **21** 382 (1975) [JETP Lett. **21**, 174 (1975)]; V.V. Anisovich, P.E. Volkovitski, and V.I. Povzun, ZhETF **70**, 1613 (1976) [Sov. Phys. JETP **43**, 841 (1976)]; A. Schmidt and R. Blankenbeckler, Phys. Rev. **D16**, 1318 (1977); F.E Close and R.G. Roberts, Z. Phys. C **8**, 57 (1981); T. Kawabe, Phys. Lett. B **114**, 263 (1982); S. Fredriksson, M. Jandel, and T. Larsen, Z. Phys. C **14**, 35 (1982).
- [57] M. Anselmino and E. Predazzi, eds., *Proceedings of the Workshop on Diquarks*, World Scientific, Singapore (1989).
- [58] K. Goeke, P.Kroll, and H.R. Petry, eds., *Proceedings of the Workshop on Quark Cluster Dynamics* (1992).
- [59] M. Anselmino and E. Predazzi, eds., *Proceedings of the Workshop on Diquarks II*, World Scientific, Singapore (1992).
- [60] U. Löring, B.C. Metsch, and H.R. Petry, Eur. Phys. J. A **10**, 447 (2001).
- [61] S. Capstick and N. Isgur, Phys. Rev. D **34**, 2809 (1986).
- [62] L.Y. Glozman, W. Plessas, K. Varga, and R.F. Wagenbrunn, Phys. Rev. D **58**, 094030 (1998).
- [63] D.V. Bugg *Four sorts of mesons* Phys. Rep. **397**, 257 (2004).
- [64] E. Klempt and A. Zaitsev, *Glueball, Hybrids, Multiquarks* (2007), <http://ftp.hiskp.uni-bonn.de/meson.pdf>.
- [65] V.V. Anisovich, Yu.D. Prokoshkin, and A.V. Sarantsev, Phys. Lett. **B389** 388 (1996), Z. Phys. A **357**, 123 (1997).
- [66] V.V. Anisovich, A.A. Kondashov, Yu.D. Prokoshkin, S.A. Sadovsky, A.V. Sarantsev, Phys. Lett. B **355**, 363 (1995).
- [67] V.V. Anisovich, A.V. Sarantsev, Phys. Lett. **382**, 429 (1996).
- [68] V.V. Anisovich, Yu.D. Prokoshkin, and A.V. Sarantsev, Phys. Lett. B **389**, 388 (1996).
- [69] V.V. Anisovich, A.A. Kondashov, Yu.D. Prokoshkin, S.A. Sadovsky,

- A.V. Sarantsev, *Yad. Fiz.* **63** 1489 (2000) [*Phys. Atom. Nucl.* **63** 1410 (2000); hep-ph/9711319].
- [70] V.V. Anisovich and A.V. Sarantsev, *Eur. Phys. J.* **A16**, 229 (2003).
- [71] A.V. Anisovich, *et al.*, *Phys. Lett.* **B 491** 47 (2000).
- [72] D. Barberis *et al.*, *Phys. Lett. B* **471**, 440 (2000).
- [73] R.S. Longacre and S.J. Lindenbaum, Report BNL-72371-2004.
- [74] V.V. Anisovich and A.V. Sarantsev, *Pis'ma v ZhETF*, **81**, 531 (2005) [*JETP Letters* **81**, 417 (2005)].
- [75] V.V. Anisovich, M.A. Matveev, J. Nyiri, and A.V. Sarantsev, *Int. J. Mod. Phys. A* **20**, 6327 (2005).
- [76] V.V. Anisovich, *Pis'ma v ZhETF*, **80**, 845 (2004) [*JETP Letters* **80**, 715 (2004)].
- [77] V.V. Anisovich and V.A. Nikonov, *Eur. Phys. J.* **A8**, 401 (2000).
- [78] V.V. Anisovich, M.N. Kobrinsky, J. Nyiri, Yu.M. Shabelski, *Quark Model and High Energy Collisions*, second edition, World Scientific, Singapore (2004).
- [79] E.M. Levin and L.L. Frankfurt, *Pis'ma v ZhETF* **2**, 105 (1965) [*JETP Letters* **2**, 65 (1965)].
- [80] H.J. Lipkin and F. Scheck, *Phys. Rev. Lett.* **16**, 71 (1966); J.J.J. Kokkedee and L. van Hove, *Nuovo Cim.* **42**, 711 (1966).
- [81] H. Satz, *Phys. Lett. B* **25** 220 (1967).
- [82] V.V. Anisovich, *Phys. Lett. B* **57**, 87 (1975).
- [83] J.W. Elbert, A.R. Erwin, W.D. Walker, *Phys. Rev. D* **3**, 2042 (1971).
- [84] V.V. Anisovich, *Strong Interactions at High Energies and the Quark-Parton Model*, in *Proceedings of the IXth LNPI Winter School*, Vol. 3, p. 106 (1974);
G. Altarelli, N. Cabibbo, L. Maiani, and R. Petronzio, *Nucl. Phys. B* **69**, 531 (1974);
T. Kanki, *Prog. Theor. Phys.* **56**, 1885 (1976);
R.C. Hwa, *Phys. Rev. D* **22**, 759, 1593 (1980);
V.M. Shekhter *Yad. Fiz.* **33**, 817 (1981) [*Sov. J. Nucl. Phys.* **33**, 426 (1981)].
- [85] V.V. Anisovich, E.M. Levin, and M.G. Ryskin, *Yad. Fiz.* **29**, 1311 (1979) [*Sov. J. Nucl. Phys.* **29**, 674 (1979)].
- [86] L.G. Dakhno and V.A. Nikonov, *Eur. Phys. J. A* **5**, 209 (1999).
- [87] V.V. Anisovich and V.M. Shekhter, *Yad. Fiz.* **28**, 1079 (1978) [*Sov. J. Nucl. Phys.* **28**, 554 (1978)].